PAGEOPH, Vol. 124, Nos. 4/5 (1986)

0033-4553/86/050659-18$1.50+0.20/0
© 1986 Birkäuser Verlag, Basel

Changes in Complex Resistivity During Creep in Granite

DAVID A. LOCKNER,[1] and JAMES D. BYERLEE[1]

Abstract—A sample of Westerly granite was deformed under constant stress conditions: a pore pressure of 5 MPa, a confining pressure of 10 MPa, and an axial load of 170 MPa. Pore volume changes were determined by measuring the volume of pore fluid (0.01 M KCl_{aq}) injected into the sample. After 6 days of creep, characterized by accelerating volumetric stain, the sample failed along a macroscopic fault. Measurements of complex resistivity over the frequency range 0.001–300 Hz, taken at various times during creep, showed a gradual increase in both conductivity and permittivity. When analysed in terms of standard induced polarization (IP) techniques, the changing complex resistivity resulted in systematic changes in such parameters as percent frequency effect and chargeability. These results suggest that it may be possible to monitor the development of dilatancy in the source region of an impending earthquake through standard IP techniques.

Key words: Complex resistivity, induced polarization, creep, earthquake.

Introduction

The electrical properties of many common rocks, composed primarily of non-conducting minerals, are controlled by the structure of pores in the rocks and by the pore fluids. Thus, any changes in pore structure, brought about by changes in fluid pressure or stress or by other processes, should have a measurable effect on the electrical response. The commonest and easiest to perform electrical experiments on rocks have measured near-dc resistivity (conductivity), as reviewed by OLHOEFT (1980) and PARKHOMENKO (1982). Important laboratory work, studying the changes in resistivity of wet rocks as a function of confining pressure, was reported by BRACE *et al.* (1965), BRACE and ORANGE (1968a), and BRACE (1971). This work was further extended to study how differential stress and sliding affect rock resistivity (BRACE and ORANGE, 1968b; BRACE, 1975). Whereas all these studies by Brace and colleagues were conducted at 10 Hz, and an additional study on unconfined granite at 2 Hz was reported by FUJII and HAMANO (1977), no one has yet measured the frequency-dependent complex resistivity response of wet rock under stress. We have undertaken the present study, along with related work (LOCKNER and BYERLEE, 1985a, 1985b), to

[1] U.S. Geological Survey, 345 Middlefield Road, Menlo Park, California 94025

expand our understanding of how earthquake processes affect the electrical response of rocks.

The measurement of resistivity changes, before and during earthquakes, received much attention when BARSUKOV (1970), SADOVSKY and NERSESOV (1972), and BARSUKOV and SOROKIN (1973) reported resistivity changes of more than 10% preceding earthquakes in the Garm region of the U.S.S.R. These findings were followed by various reports of smaller anomalies preceding earthquakes and, finally, observations of as much as 14% resistivity change before a magnitude 4 earthquake (MAZZELLA and MORRISON, 1974) on the San Andreas fault in California. Although these results were encouraging, calculations indicated (HANKS, 1974; MORRISON *et al.*, 1977) that the volumetric strains required to produce changes in resistivity of this magnitude should also have resulted in easily observable uplifts and tilts. Significant problems still remain in discriminating earthquake-related resistivity changes from background noise (i.e., changes in resistivity due to ground-water-level fluctuations), although progress has been made in this area (MORRISON and FERNANDES, (1986)).

A variety of techniques have been used to monitor resistivity changes related to earthquakes. These techniques include active dipole–dipole measurements, such as those used by Morrison, as well as techniques based on changes in electrical potential induced by magnetotelluric currents. The laboratory results presented in this paper suggest that an additional measurement technique, which has not yet been exploited, may be to monitor the change in induced polarization (IP) in the source region of an earthquake.

IP response has been used extensively in the mining industry in prospecting for disseminated sulfides and other ore bodies (MADDEN and CANTWELL, 1967; SUMNER, 1976). This technique is based on the fact that at frequencies below approximately 1 kHz, some ore bodies exhibit strong polarizaton effects, resulting in measurable out-of-phase currents. These polarization effects are related to grain-electrolyte interactions and occur to some extent in almost all wet rocks (WAIT, 1959; LOCKNER and BYERLEE, 1985a, 1985b). Because this low-level response is unwanted when prospecting for mineral deposits, it is known as 'background' IP response, and also occurs in clays and other fault-gouge materials (ARULANANDAN and MITCHELL, 1968; OLHOEFT, 1979a, 1985; LOCKHART, 1980; LOCKNER and BYERLEE, 1985b). Not only would measurement of the IP response of earthquake source regions include the near-dc resistivity response currently being studied, but it would also extend this measurement to include the full frequency-dependent complex resistivity response of the fault zone and could eventually be extended to study the nonlinear response reported for clays (OLHOEFT, 1979a).

Although we can expect stress and strain changes to significantly affect the complex resistivity of rock, very few quantitative data exist relating these parameters to each other. Many of the mechanisms responsible for the out-of-phase currents occurring below 1,000 Hz are related to rock-electrolyte interactions at the

pore surfaces. Thus, any changes in microcrack surface area, due to changes in stress or strain within an earthquake source region, may result in measurable phase changes in the complex resistivity. Because the current which is in phase with the electrical potential is related primarily to the cross-sectional area of the interconnected pore structure, comparison of in-phase and out-of-phase currents may reveal useful informaton about changes in the pore structure of the rock. The rest of this report is concerned with laboratory measurements of the complex resistivity of saturated rocks when loaded hydrostatically and triaxially, as well as with the implications that these measurements have for the field of earthquake prediction.

We will make use of the following parameters: complex resistivity $\rho^* = \rho' - i\rho''$, where $i = (-1)^{1/2}$, complex conductivity $\sigma^* = \sigma' + i\sigma''$ and complex relative permittivity $K^* = K' - iK''$. These parameters are related by

$$\sigma^* = i\omega\varepsilon_0 K^* = (\rho^*)^{-1}, \tag{1}$$

where $\omega = 2\pi f$ is the angular frequency and ε_0 is the permittivity of free space. Then, the dissipation factor D or loss tangent $\tan \delta$ is given by

$$D = \tan \delta = \sigma'/\sigma'' = \rho'/\rho'' = K''/K'. \tag{2}$$

We also define the phase angle $-\varphi$ by which current leads voltage, so that $\varphi = \delta - \pi/2$. We have made no distinction here as to the mechanisms that result in the observed frequency response. Therefore, the parameters sometimes referred to as effective conductivity and effective permittivity are here symbolized by σ' and K', respectively.

Experimental Method

The measurement system that we have used employs a four-electrode technique, described in detail in LOCKNER and BYERLEE (1985a) and was first developed by OLHOEFT (1979b, 1985).

A nominal 0.5-V p − p sinewave input signal was provided to the sample (Figure 1) across the outer pair of electrodes (one electrode was electrically grounded to the system through the pore fluid), using a Crown[1] DC-300A amplifier. The voltage drop across the sample was measured with an Intronics IA294 high input impedance ($3 \times 10^8\ \Omega$) isolation amplifier with a low-noise-current and an active-driven shield. Corrections were made for the voltage drop across the thin Al_2O_3 wafers contacting the sample (Figure 2). The current was determined by monitoring the voltage drop across a precision decade resistor placed in series with the sample. By sampling the

[1] Any use of trade names and trademarks in this report is for description purposes only and does not constitute endorsement by the U.S. Geological Survey.

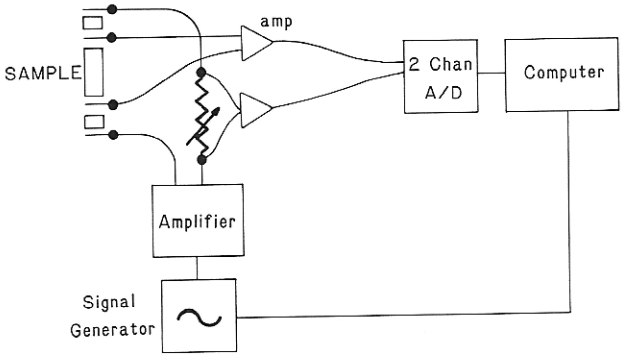

Figure 1
Schematic diagram of four-electrode system used to measure complex resistivity.

voltage and current 128 times per cycle, the magnitude and phase of the sample resistivity were calculated, along with harmonic distortion and system noise. Resistivity was measured with this system at discrete frequencies between 0.001 and 300 Hz.

A cylindrical sample of Westerly granite, 25.4 mm in diameter and 52.1 mm long was used in this experiment. The sample was presaturated with 0.01 *M* KCl in distilled, deionized water by first evacuating the sample for 24 h and then submerging it in the electrolyte for an additional 24 h at 0.7 MPa pressure. The KCl solution (resistivity, 6.5 Ω-m at 28.5°C) was used primarily for comparison of the results with those of earlier experiments (LOCKNER and BYERLEE, 1985a, 1985b). The sample was jacketed in vinyl tubing (Figure 2) and sandwiched between 0.51-mm-thick porous Al_2O_3 wafers, Pt screen electrodes, 2.36-mm-thick porous Al_2O_3 spacers, Pt screen electrodes, and, finally, 25.4-mm-thick nonporous Al_2O_3 spacers. Pt wires, contacting the electrodes, were passed through the jacket (sealed with vinyl cement) and crimp-connected to four leads brought out of the pressure vessel. Pore fluid was connected through a hole in the upper Al_2O_3 spacer with a precision pore pressure system, capable of resolving a 0.2-mm^3 change in pore volume, or a volumetric strain of 10^{-5}. The sample and pore pressure system were housed in a temperature-controlled chamber at 28.5 ± 0.2°C.

The sample assembly was placed in a pressure vessel and maintained at 10.0 ± 0.2 MPa confining pressure and 5.0 ± 0.1 MPa pore pressure. After 20 h, there was no detectable change in pore volume. At that time, axial load was raised at a constant rate for 19 h to 170 ± 1 MPa. Equipment problems forced the sample to be removed after 22 h. The confining and pore pressures were then reapplied for another 24 h, at which time the sample had reequilibrated and the experiment resumed. Resistivity measurements were made under hydrostatic conditions, and then an axial stress of 170 MPa was rapidly applied. The sample was held at this constant stress until, approximately 6 days later, it failed. Resistivity was repeatedly

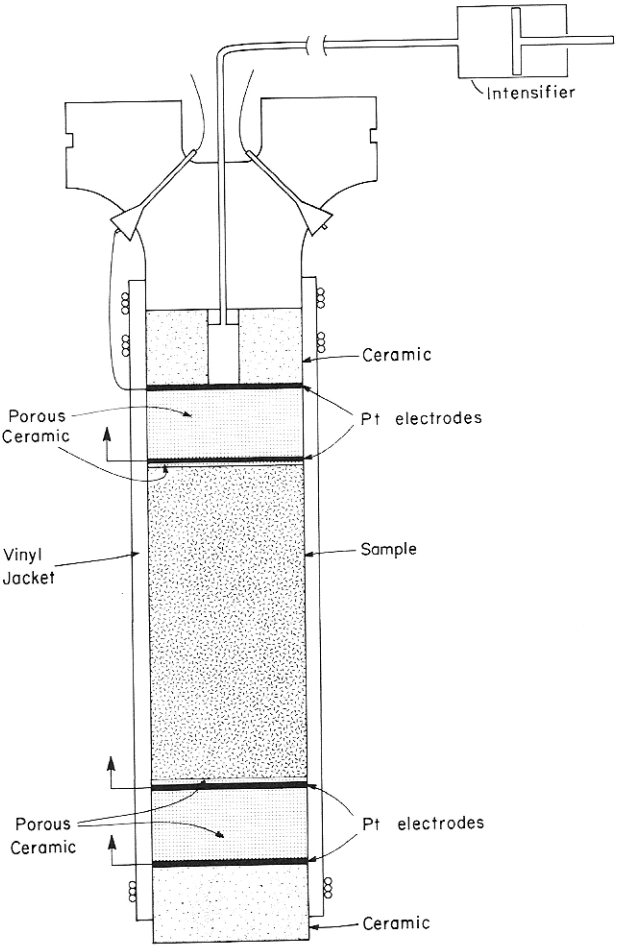

Figure 2
Sample assembly. Differential stress is applied by advancing piston against end of sample column.

measured over the entire duration of the creep experiment. Because the sample was deforming under deviatoric stress conditions, we expected a significant anisotropy to develop in the resistivity over the course of the experiment. However, we measured resistivity only parallel to the direction of maximum principal stress.

The sample resistance was measured to $\pm 0.05\%$ accuracy; however, uncertainties in the sample dimensions reduced the absolute accuracy of resistivity measurements to $\pm 0.1\%$. Phase angle measurements were accurate to ± 0.3 mrad.

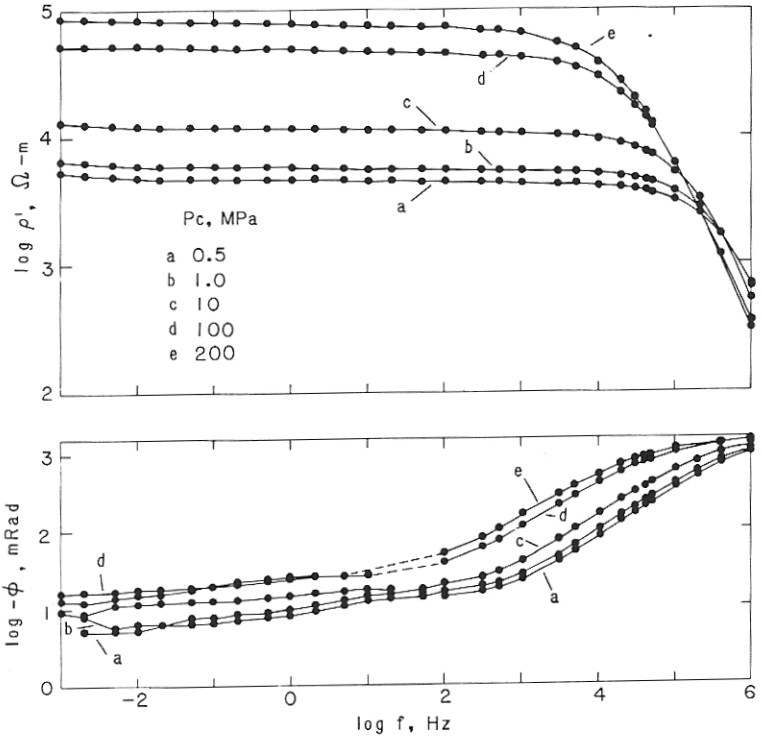

Figure 3

log ρ' and log-φ versus log f for Westerly granite loaded at selected confining pressures (from LOCKNER and BYERLEE, 1985a). In the present creep experiment, all measurements are below 300 Hz.

Results

Hydrostatic experiments

Frequency-dependent resistivity data can be presented in various ways. In general, a pair of parameters, e.g., (ρ', ρ'') or (ρ', φ), are required to present the complete resistivity. For example, we plot data, first reported in LOCKNER and BYERLEE (1985a), obtained during hydrostatic loading of a sample of Westerly granite. Whereas we measure resistivity at frequencies only as high as 300 Hz in the present creep experiment, additional equipment was used in the hydrostatic experiments that allowed us to extend the frequency range to 10^6 Hz. Thus, in Figure 3, log ρ' and log $-\varphi$ are plotted as functions of log frequency for selected confining pressures as high as 200 MPa. Measurements were taken in order of increasing confining pressure with the pore pressure system vented to the atmosphere. As expected, ρ' increases with increasing confining pressure as the pore volume is reduced. At frequencies below 1 kHz, log ρ' shows only a slight frequency dependence, whereas above 1 kHz, log ρ' decreases rapidly, and φ approaches $-\pi/2$ as the sample behaves

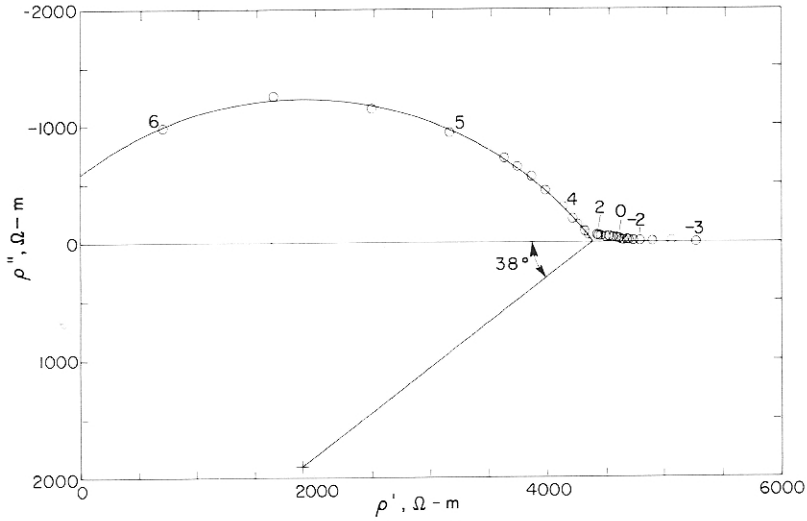

Figure 4

Argand diagram for Westerly granite at 0.5 MPa confining pressure (from LOCKNER and BYERLEE, 1985a). Numbers denote log frequency for selected frequencies. High-frequency ($f > 1$ kHz) data show Cole–Cole response whereas primary feature of low-frequency data is dispersion.

more like a dielectric. We note that even at 10^{-3} Hz, $\varphi \sim -10$ mrad, and approximately 1% of the current is out of phase with the voltage.

An Argand diagram, in which ρ'' is plotted versus ρ', can be a useful way of viewing resistivity data. Figure 4 is an Argand diagram of the granite data measured at 0.5 MPa. Data above 1 kHz fall on a circular arc whose center is depressed below the real axis. This feature can be modeled by a circuit containing a distribution of relaxation-time constants (Cole–Cole distribution (COLE and COLE, 1941)) of the form

$$K^* = K_\infty + \frac{K_0 - K_\infty}{1 + (i\omega\tau)^{1-\alpha}}, \qquad (0 \leqslant \alpha \leqslant 1) \tag{3}$$

where K_0 and K_∞ are the low- and high-frequency limits, respectively, of relative permittivity and α is the Cole–Cole distribution parameter. Below 1 kHz, the data no longer fit the Cole–Cole model, and, instead, the principal feature is strong dispersion of ρ'. One consequence of this behavior is that the practical definition of dc resistivity ρ'_{dc} becomes ambiguous. In the present creep experiment, we measure resistivity only as high as 300 Hz. Thus, we observe only low-frequency dispersion phenomena and not the Cole–Cole style response. Although the high-frequency response contains useful information, it is not generally measurable in large-scale IP field studies because, under these conditions, inductive coupling effects commonly dominate the response above 1 kHz.

Creep experiment

To study how time-dependent crack growth affects complex resistivity, we conducted a creep experiment on a sample of Westerly granite. In this experiment, constant stress conditions of 10.0 MPa confining pressure, 5.0 MPa pore pressure, and 170 MPa axial load were applied to the sample until, after 6 days, it failed. Representative data, measured 61,200 s (17.0 h) into the creep experiment, are plotted versus log frequency in Figure 5. A decrease in ρ' by approximately 15% over the measured frequency range during this part of the experiment resulted in a nearly linear decrease of 2.7% per decade of frequency. As the sample approached failure, resistivity change decreased to 1.8% per decade of frequency. Because the phase angle is relatively small (-35 to -15 mrad), $\sigma' \simeq 1/\rho'$. A least-squares fit of the form $\log \sigma' = a + m \log_{10} f$ gives: $a = -3.4052 \pm 0.0003$ and $m = 0.0128 \pm 0.0002$. The frequency dependence of σ' systematically decreased to $m = 0.009$ at failure. ρ'' essentially follows the phase angle $-\varphi$, which gradually increases with frequency. Phase angle is relatively featureless and displays a broad plateau in the range 0.01 to 10 Hz. This result agrees with measurements of complex resistivity of Westerly granite under hydrostatic conditions (Figure 3). Finally, the slowly varying real resistivity and the nearly constant phase angle result in a real permittivity K' that falls off at approximately ω^{-1} (Figure 5). This strong low-frequency dispersion results in large values of K', e.g., $K' = 10^8$ at 0.001 Hz.

Whereas the magnitude of ρ^* varied systematically during the creep experiment, the relative form of the frequency dependence of both ρ' and ρ'' was remarkably stable. In fact, other than the gradual decrease in the slope of $\rho'(\omega)$ already mentioned, the relative form of the frequency dependence remained constant to within experimental error, including during the initial period when the sample was loaded hydrostatically.

We found that both σ' and K' increased monotonically during the creep experiment. Although we expected that σ' should increase as dilatancy progressed, a concomitant increase in K' has never before been reported. The relative changes in σ' and K' are plotted in Figure 6. Each point represents the change in σ' and K', at 1 Hz, relative to the value measured at the start of creep. Failure occurred 512,320 s (5.93 d) after differential stress was applied. The values of σ' and K', at 1 Hz, before application of differential stress ($p_c = 10$ MPa, $p_p = 5$ MPa) were 2.31×10^{-4} S/m and 0.92×10^5, respectively. The volumetric strain during creep (determined from measurement of the pore volume increase), as well as the axial shortening, are plotted as the lower curves of Figure 6. The sample displayed the three classic modes of creep. Rapid, exponentially decaying primary creep lasted a few thousand seconds, followed by 3 to 4 days of secondary creep, in which strain rate was nearly constant. Finally, the sample underwent a smooth transition to tertiary creep, characterized by continually increasing strain rate and ending in macroscopic failure (Figure 7). A single throughgoing fault formed at failure, making an angle of 20° with the axis of

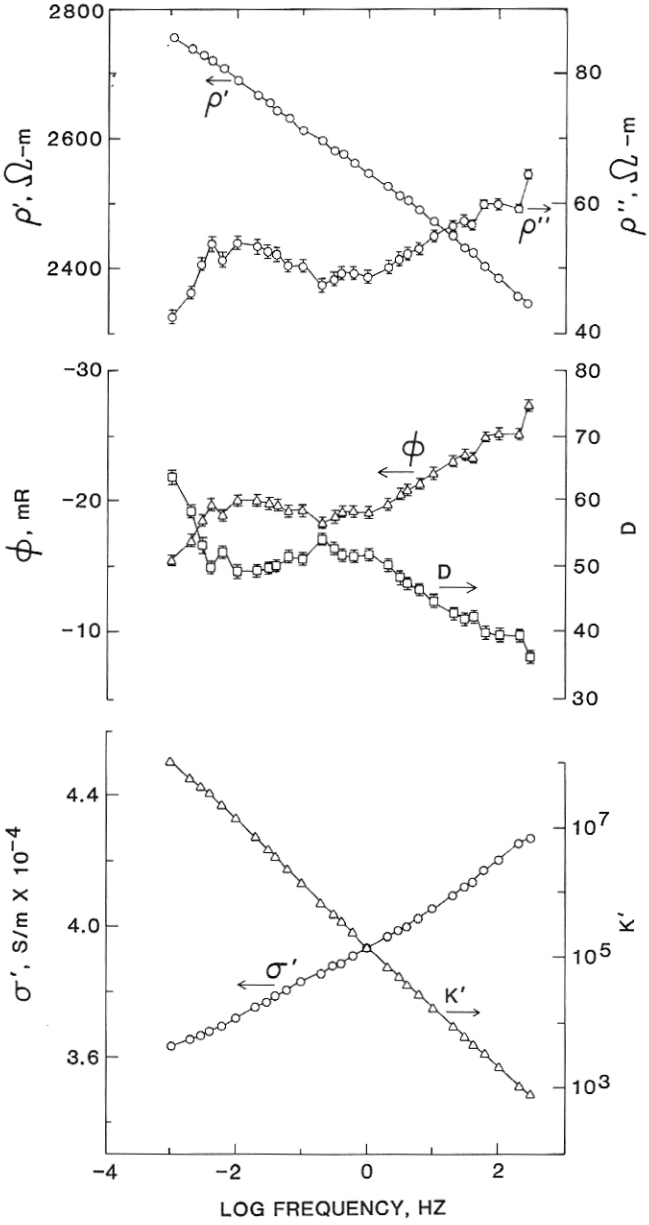

Figure 5
Resistivity parameters for sample 61,200 s after start of creep. Where no error bars are drawn, errors are smaller than the size of the symbols.

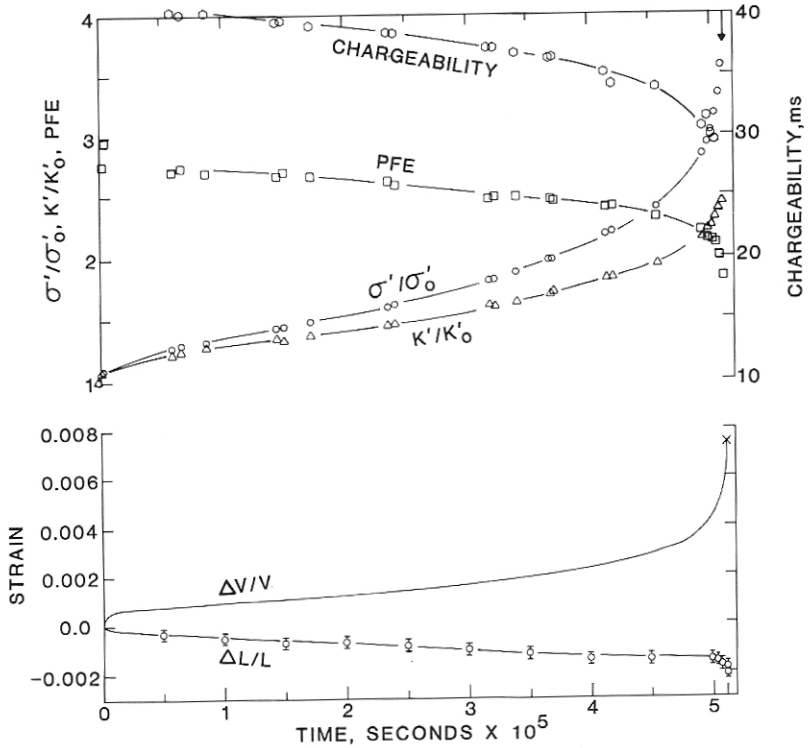

Figure 6

Changes in various parameters during creep. Changes in σ' and K' (at 1 Hz) are plotted relative to starting values. At $t = 0$, $\sigma' = 3.08 \times 10^{-4}$ S/m and $K' = 1.08 \times 10^5$. Percent frequency effect (PFE) and chargeability ($M_{0.01,1.0}^{12.5}$) are parameters used in IP studies. Arrow denotes time of failure of sample (512, 360 s).

the sample. The sample shortened 0.2% over the duration of the creep experiment, whereas volumetric strain due to creep reached 0.75% at failure; more than half of this strain occurred during tertiary creep.

Discussion

The primary studies of stress-related changes in the resistivity of wet rocks (BRACE and ORANGE, 1966; BRACE and ORANGE, 1968b) measured real resistivity ρ' at 10 Hz as the samples were stepped through increasing stress levels leading to failure. Nearly all samples showed the same general behavior. At low stress, conductivity decreased with applied stress as existing cracks closed. Eventually, as stress increased to the level at which new cracks began to form, allowing fluid to flow back into the rock, conductivity increased to failure. FUJII and HAMANO (1977) measured changes in resistivity at a frequency of 2 Hz in a granite sample, initially 50% saturated, and

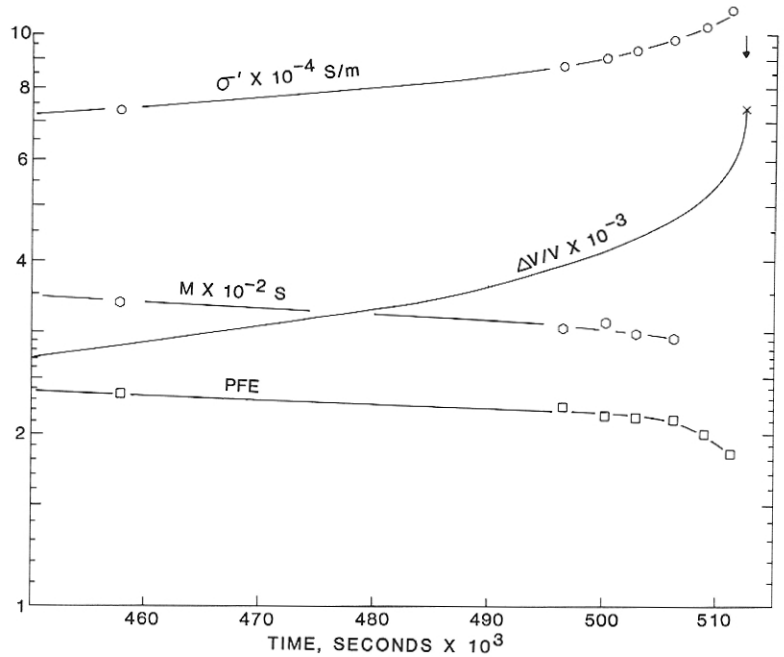

Figure 7
Real conductivity at 1 Hz (σ'), percent frequency effect (PFE), chargeability (M), and volumetric strain ($\Delta V/V$) versus time for final 17 h of experiment. Arrow denotes time of failure of sample.

cycled under uniaxial compression. Their results are difficult to interpret since any change in pore volume, either an increase of a decrease, tended to reduce resistivity both parallel and perpendicular to the loading axis. Therefore, we compare our results only with those of Brace and Orange. In our experiment, we chose to measure resistivity at constant stress so as to remove effects related to changing crack geometry in response to stress changes. Thus, we measured the effects due only to dilatant cracking, and have extended our measurements to both real and imaginary resistivity over a broad frequency range.

As shown in Figure 5, real conductivity varied systematically with frequency over the entire creep experiment; i.e., $\sigma' \propto \omega^{0.013}$ at the beginning of creep and gradually changed to $\sigma' \propto \omega^{0.009}$ by the time of failure. This relation could not be observed by earlier experimenters, although, in the hydrostatic experiments on Westerly granite and Berea sandstone reported above, we measured exponents of 0.009 ± 0.003 and 0.0045 ± 0.003, respectively. With data of poorer quality or spanning a smaller frequency range, it becomes difficult to estimate this small frequency dependence directly. In this case, the asymptotic relation derived by DISSADO and HILL (1984) and discussed by LOCKNER and BYERLEE (1985a),

$$\frac{K' - K_\infty}{K''} = \tan\left[\frac{\pi}{2}(1 - p)\right], \tag{4}$$

where K_∞ is the high-frequency limit of relative permittivity, is useful. Since this equation is derived, in part, from the relation

$$K'' \propto \omega^{-p}, \tag{5}$$

we combine expression (5) with

$$\sigma' = i\omega\varepsilon_0 K'' \tag{6}$$

to obtain

$$\sigma' \propto \omega^{1-p}. \tag{7}$$

For $K' \gg K_\infty$,

$$1 - p = -\frac{2\varphi}{\pi}. \tag{8}$$

Thus, for rock-electrolyte systems that obey the low-frequency dispersion model of DISSADO and HILL (1984), in the region below the critical frequency, the frequency dependence of σ' will be directly related to phase angle:

$$\sigma' \propto \omega^{-\frac{2\varphi}{\pi}}. \tag{9}$$

In our hydrostatic experiments, we found that the critical frequency decreased from 68 kHz at 0.5 MPa to 1.4 kHz at 200 MPa confining pressure. In the creep experiment data shown in Figure 5, the steady increase in phase angle above 10 Hz indicates an approach to the critical frequency.

In IP measurements and other field applications of electrical resistivity, it is commonly assumed that the low-frequency conductivity (or resistivity) of rock levels off at a limiting value $\sigma_{dc} = 1/\rho_{dc}$. From our creep experiment, as well as from our hydrostatic experiments, σ_{dc} may not always be a well-defined quantity (Figures 4 and 5), especially in materials that exhibit strong low-frequency dispersion of permittivity (JONSCHER, 1978; DISSADO and HILL, 1984). The slowly varying real resistivity and the nearly constant phase angle result in a real permittivity K' that falls off at approximately ω^{-1}. This feature is important in distinguishing a sample exhibiting a strong low-frequency dispersion response from a sample with a finite σ_{dc}. The strong low-frequency dispersion model suggested by Dissado, Hill, and Jonscher predicts that both K' and K'' are nearly proportional to ω^{-1}. Since σ_{dc} transforms to $K'' \propto \omega^{-1}$, these two models can be distinguished only by the K' response. In this case, constant K' would indicate a dc conduction model, whereas $K' \propto \omega^{-1}$, as in our experiments, agrees with the low-frequency dispersion model.

The observed changes in conductivity and permittivity are related principally to

the deformation and growth of fluid-filled pores as the sample became increasingly dilatant. Archie's law is a well-known empirical relation between conductivity and porosity:

$$F = v^{-r}, \tag{10}$$

where v is porosity and r is an exponent generally in the rage 1–2. The formation factor F is defined as the ratio σ (electrolyte)/σ (saturated rock). BRACE *et al.* (1965) found that for various rocks at confining pressures from 400 to 1,000 MPa, r = 2 provided a good fit, whereas r generally decreased for confining pressures below 400 MPa, at which pressure crack porosity in crystalline rocks is important. In our hydrostatic experiments (LOCKNER and BYERLEE, 1985a), we estimated $r = 1.3$ for Westerly granite at 1 MPa, increasing to $r = 2.1$ at 200 MPa, whereas for Berea sandstone, $r = 1.6$ and was independent of confining pressures as high as 200 MPa. Consequently, our hydrostatic data, as well as those of BRACE *et al.* (1965), show a tendency for r to decrease as the population of low-aspect-ratio (long and narrow) cracks increases.

In the current experiment, we measured pore-volume changes directly and thus can look for changes in r during creep. However, we could not accurately measure the pore volume at the start of the creep experiment, so we must estimate its value. Assuming a total porosity at the start of creep of $v = 0.006 \pm 0.002$, r smoothly decreases from an initial value of 1.19 ± 0.07 until, at the time of failure, $r = 1.11 \pm 0.04$, as shown in the upper curve of Figure 8. The solution to Archie's law for $r = 1.19$, fitting the conductivity data at the start of creep, is also plotted. Migration of the conductivity data above this line as creep progresses, indicates the trend toward lower r. Although quantitative data do not yet exist that would allow us to relate conductivity changes to the geometry and number of microscopic pores in rocks, a limited number of studies of this nature have been conducted. In general, it is found (KRANZ, 1979; TAPPONNIER and BRACE, 1976; HADLEY, 1976) that the development of dilatancy in stressed rock is accompanied by an increase in the number of microcracks, as well as by a shift in the crack population toward low-aspect-ratio cracks. If we assume that this same process of development of low-aspect-ratio cracks, observed by Kranz in his creep experiments, occurred in our sample, then we also observed decreasing r with increasing number of low-aspect-ratio cracks.

The variations of σ' and K' with creep (Figures 6 and 7) may have interesting field applications. Both frequency-domain resistivity measurements, similar to the laboratory measurements reported here, and time-domain measurements are being performed in the field; primarily in IP studies. Because the granite sample behaved linearly at the low current densities used in our experiment (0.001–0.004 A/m^2), we can use our frequency measurements to calculate the time-domain response of the sample (LOCKNER and BYERLEE, 1985b]. Current density $\mathbf{J}(\omega)$ is related to electric field $\mathbf{E}(\omega)$ by the complex resistivity, referred to in this context as the system transfer function:

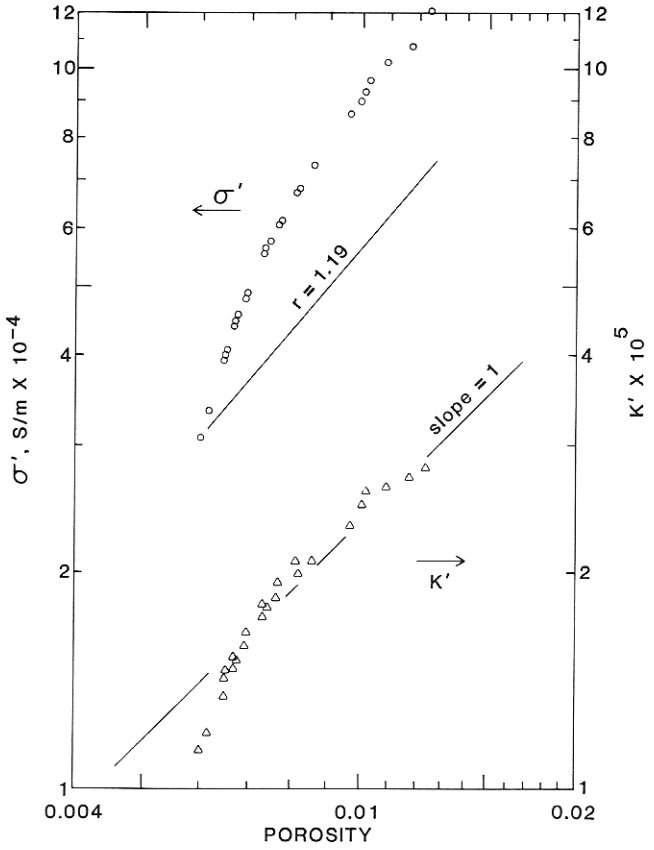

Figure 8
log σ' and log K' versus log v during creep experiment (creep progressed from left to right). Initial porosity is estimated at 0.006 ± 0.002.

$$\mathbf{E}(\omega) = \rho^*(\omega)\mathbf{J}(\omega). \tag{11}$$

For a given input signal $\mathbf{j}(t)$, we take the discrete Fourier transform (DFT) to obtain its frequency content $\mathbf{J}(\omega)$, multiply by $\rho^*(\omega)$, and then take the inverse transform to obtain the electric field time response $\mathbf{e}(t)$:

$$\mathbf{e}(t) = \mathrm{DFT}^{-1}\{\rho^*(\omega)\mathrm{DFT}(\mathbf{j}(t))\}. \tag{12}$$

For example, we use a square-wave input current function of 100-s period, where

$$\mathbf{j}(t) = \begin{cases} 0, & (0 < t < 37.5) \\ -1, & (37.5 < t < 50) \\ 0, & (50 < t < 87.5) \\ 1, & (87.5 < t < 100) \end{cases} \tag{13}$$

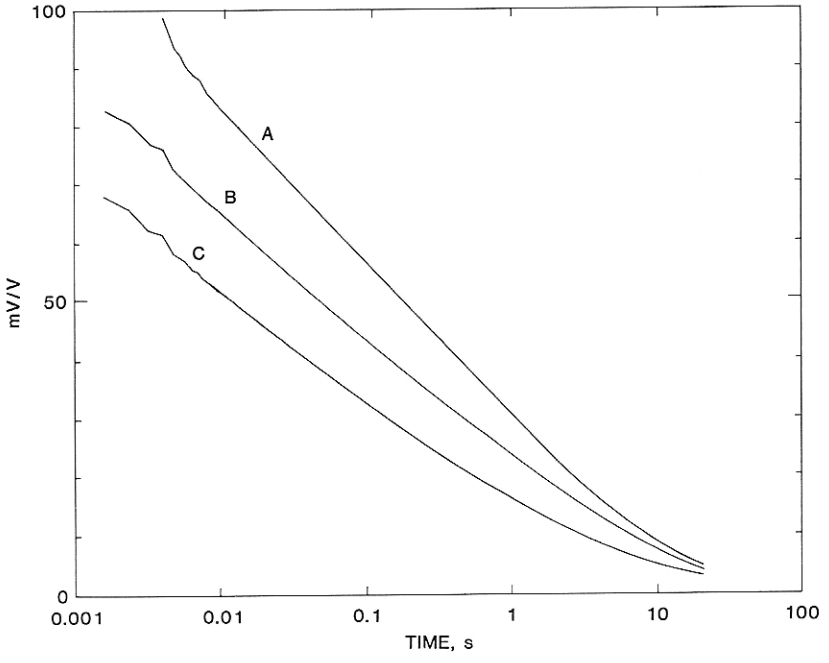

Figure 9
IP decay curves, calculated from $\rho^*(\omega)$ data, are plotted for various times after start of creep: A, 61,200 s; B, 496,500 s; C, 511, 270 s. Curves represent voltage decay following shutoff of a 12.5-s-duration constant-current pulse. Gradual decrease in decay curve as sample approached failure reflects decrease in chargeability M.

The input function is divided into 2^{17} equal time steps to obtain 5 orders-of-magnitude of dynamic range in time. Results of successive stages of the creep experiment are plotted in Figure 9. As is common in IP response (SUMNER, 1976), the voltage decays nearly linearly over much of the record. As dilatancy increases, the voltage decay becomes progressively faster, even though each decay curve is plotted relative to the maximum voltage for that run, so that the effects due to changes in the near-dc conductivity are removed. In IP studies, this effect is quantified by the percent frequency effect (PFE), which is defined as the percent drop in resistivity per decade of frequency (Figures 6 and 7). PFE shown in these figures is calculated using values of ρ' at 0.1 and 10 Hz. Near the end of the experiment, where ρ' was changing rapidly, a significant decrease in resistivity would occur over the time required to perform the low-frequency measurements. Corrections for this effect have been made. Another parameter commonly used in IP analysis is the chargeability, $M^{t1}_{t2,t3} = \frac{1}{U_0}\int_{t^2}^{t_3} U dt$, where $t1$ is the interval over which current is driven through the ground and U is the potential. Computed values of $M^{12.5}_{0.01,1.0}$ are also plotted in Figures 6 and 7. Because changes in decay time, PFE, and chargeability can be detected by

standard IP techniques, the changes in these parameters, as the sample approached failure, suggest that measurements of this type may be useful as intermediate-or short-term earthquake prediction tools. By measuring secular changes in the IP response of the source region of an impending earthquake, it may be possible to monitor prefailure volume changes of this region. Such a field experiment might include downhole electrodes, possibly straddling the fault, to minimize the effects of water-table fluctuations and surface noise, and to sample resistivities at the greatest possible depth while minimizing inductive coupling problems.

During most of the creep experiment, relative changes in K', PFE, and M were about one-half to three-quarters the relative change observed in conductivity. Therefore, unless these parameters can be measured more easily or more accurately than conductivity, they might be only of supplementary value for field applications under conditions similar to this creep experiment. However, rocks that show a stronger IP response than the granite used in this experiment may show more dramatic stress- or volume-related changes. Additional laboratory experiments are currently underway to test this hypothesis.

Conclusions

Ongoing efforts to predict earthquakes through detection of changes in apparent resistivity are based on measurements of near-dc resistivity. Recent laboratory measurements of frequency-dependent magnitude and phase relations of the resistivity of wet rock suggest that monitoring full complex resistivity in the field may provide a new tool for predicting earthquakes. In the laboratory data, the principal changes in the electrical response of saturated granite, during creep at constant stress, are systematic increases in σ' and K' over time. Whereas the increase in σ' would be reflected in the σ_{dc} measurements currently being performed in the field, K' is not being measured.

While the increase in σ' in laboratory measurements is due primarily to an increase in pore volume, we suggest that the increase in K' is related to increasing surface area as microcracks grow in the sample. These results suggest the possibility of using standard IP measurement techniques to monitor dilatancy-related changes in an earthquake source region, as an intermediate- or short-term predictive tool.

References

ARULANANDAN, K. and MITCHELL, J. (1968), *Low frequency dielectric dispersion of clay-water-electrolyte systems.* Clay and Clay Minerals *16*, 337–351.

BARSUKOV, O. M. (1970), *Relationship between the electrical resistivity of rocks and tectonics processes.* Bull. (Izv) Acad. Sci. U.S.S.R., Earth Physics *1*, 55.

BARSUKOV, O. M. and SOROKIN, O. N. (1973), *Variations in apparent resistivity of rocks in the seismically active garm region.* Bull. (Izv) Acad. Sci. U.S.S.R., Earth Physics *10*, 685.

BRACE, W. F., ORANGE, A. S. and MADDEN, T. R. (1965), *The effect of pressure on the electrical resistivity of water-saturated crystalline rocks.* J. Geophys. Res. *70*, 5669–5678.

BRACE, W. F. and ORANGE, A. S. (1966), *Electrical resistivity changes in saturated rock under stress,* Science *153*, 1525–1526.

BRACE, W. F. and ORANGE, A. S. (1968a), *Further studies of the effects of pressure on electrical resistivity of rocks.* J. Geophys. Res. *73*, 5407–5420.

BRACE, W. F. and ORANGE, A. S. (1968b), *Electrical resistivity changes in saturated rocks during fracture and frictional sliding.* J. Geophys. Res. *73*, 1433–1445.

BRACE, W. F. (1971), *Resistivity of saturated crustal rocks to 40 km based upon laboratory measurements in the structure and physical properties of the Earth's crust.* Geophys. Monogr. Ser. *14*, edited by J. G. Heacock, 243–255, AGU, Washington, D.C.

BRACE, W. F. (1975), *Dilatancy related electrical resistivity changes in rocks.* PAGEOPH *113*, 207–217.

COLE, K. S. and COLE, R. H. (1941), *Dispersion and adsorption in dielectrics, I. Alternation current characteristics.* J. Chem. Phys. *9*, 341–351.

DISSADO, L. A. and HILL, R. M. (1984), *Anomalous low-frequency dispersion.* J. Chem. Soc. Faraday Trans. 2 *80*, 291–319.

FUJII, N. and HAMANO, Y., *Anisotropic changes in resistivity and velocity during rock deformation.* In *High Pressure Research, Applications in Geophysics* (ed. Manghnani, M. H., and Akimoto, S-I.) (Academic Press, Inc., New York 1977) pp. 53–63.

HADLEY, K. (1976) *Comparison of calculated and observed crack densities and seismic velocities of Westerly granite.* J. Geophys. Res. *81*, 3484–3494.

HANKS, T. C. (1974) *Constraints on the dilatancy-diffusion model of the earthquake mechanism.* J. Geophys. Res. *79*, 3023–3025.

JONSCHER, A. K. (1978) *Low-frequency dispersion in carrier-dominated dielectrics.* Philos. Mag. B *38*, 587–601.

KRANZ, R. L. (1979), *Crack growth and development during creep of Barre granite.* Int. J. Rock Mech. Min. Sci. *16*, 23–35.

LOCKHART, N. C. (1980), *Electrical properties and the surface characteristics and structure of clays, I. Swelling clays.* J. Colloid and Interface Sci. *74*, 520–529.

LOCKNER, D. A. and BYERLEE, J. D. (1985a), *Complex resistivity measurements of confined rocks.* J. Geophys. Res. *90*, 7837–7847.

LOCKNER, D. A. and BYERLEE, J. D. (1985b), *Complex resistivity of fault gouge and its significance for earthquake lights and induced polarization.* Geophys. Res. Lett. *12*, 211–214.

MADDEN, T. and CANTWELL, R. (1967), *Induced polarization, a review.* Min. Geophys. *2*, 373–400.

MAZZELLA, A. and MORRISON, H. F. (1974), *Electrical resistivity variations associated with earthquakes on the San Andreas fault.* Science *185*, 855–857.

MORRISON, H. F., CORWIN, R. F. and CHANG, M. (1977), *High-accuracy determination of temporal variations of crustal resistivity.* Amer. Geophys. Union Monogr. 20, The Earth's Crust.

MORRISON, H. F. and FERNANDES, R. (1986), *Temporal variations in the electrical resistivity of the Earth's crust.* J. Geophys. Res., *91*, 11618–11628.

OLHOEFT, G. R., *Nonlinear electrical properties, In Nonlinear Behavior of Molecules, Atoms and Ions in Electric, Magnetic or Electromagnetic Fields* (ed. Neel, L.) (Elsevier, Amsterdam 1979a) pp. 395–410.

OLHOEFT, G. R. (1979b), *Electrical properties, initial reports on the Petrophysics laboratory.* U.S. Geol. Surv. Circ. *789*, 1–25.

OLHOEFT, G. R., *Electrical properties of rocks,* In *Physical Properties of Rocks and Minerals,* chap. 9 (eds. Touloukian, Y. S., Judd, W. R. and Roy, R. F.) (McGraw-Hill, New York 1980).

OLHOEFT, G. R. (1985), *Low frequency electrical properties.* Geophys. *50*, 2492–2503.

PARKHOMENKO, E. I. (1982), *Electrical resistivity of minerals and rocks at high temperature and pressure.* Rev. Geophys. and Space Phys. *20*, 193–218.

SADOVSKY, M. A., NERSESOV, I. L., NIGMATULLAEV, S. K., LATYNINA, L. A., LUKK, A. A., SEMENOV, A. N., SIMBIREVA, I. G., and ULOMOV, V. I. (1972), *The processes preceding strong earthquakes in some regions of Middle Asia.* Tectonophysics *14*, 295–307.

SUMNER, J. S., *Principles of Induced Polarization for Geophysical Exploration* (Elsevier Scientific Publ. Co., New York 1976) p. 277.

TAPPONNIER, P. and BRACE, W. F. (1976), *Development of stress-induced microcracks in Westerly granite.* Int. J. Rock Mech. Min. Sci. *13*, 103–112.

WAIT, J. R. (Ed.), *Overvoltage Research and Geophysical Applications* (Pergamon Press 1959).

(Received November 1, 1985, revised/accepted June 28, 1986)